

UNCOVERING THE HUMAN MOTION PATTERN: PATTERN MEMORY-BASED DIFFUSION MODEL FOR TRAJECTORY PREDICTION

Yuxin Yang, Pengfei Zhu, Mengshi Qi, Huadong Ma

Beijing Key Laboratory of Intelligent Telecommunications Software and Multimedia,
Beijing University of Posts and Telecommunications

ABSTRACT

Human trajectory forecasting is a critical challenge in fields such as robotics and autonomous driving. Due to the inherent uncertainty of human actions and intentions in real-world scenarios, various unexpected occurrences may arise. To uncover latent motion patterns in human behavior, we introduce a novel memory-based method, named **Motion Pattern Priors Memory Network**. Our method involves constructing a memory bank derived from clustered prior knowledge of motion patterns observed in the training set trajectories. We introduce an addressing mechanism to retrieve the matched pattern and the potential target distributions for each prediction from the memory bank, which enables the identification and retrieval of natural motion patterns exhibited by agents, subsequently using the target priors memory token to guide the diffusion model to generate predictions. Extensive experiments validate the effectiveness of our approach, achieving state-of-the-art trajectory prediction accuracy. The code will be made publicly available.

Index Terms— Trajectory Prediction, Memory Network, Clustering, Diffusion Model

1. INTRODUCTION

Human trajectory prediction plays a pivotal role in ensuring the safety and efficiency of applications such as autonomous driving systems [1] and social robots. However, predicting human trajectories is inherently challenging due to the unpredictable and subjective nature of human behavior.

To solve these challenges, significant strides have been achieved in research across different aspects, such as social interactions modeling [2, 3]. To emphasize the capability of accurately forecasting a wide range of potential future trajectories in various situations, many generative models are utilized for stochastic trajectory prediction to model the distribution of future trajectories, including generative adversarial networks (GANs)-based[4], conditional variational autoencoder (CVAE)-based [5, 6, 7], and diffusion-based [8] methods. Recently, memory networks have been used in the task of trajectory prediction. Many approaches create memory repositories with different contents. Some methods [6, 9] store all

trajectories or clusters of trajectories in the memory bank, and the selection for prediction simply relies on calculating cosine similarity between observed and stored trajectories. Other methods [10] use memory mechanisms by storing starting and ending points and training a scoring network to select appropriate intentions.

While notable advancements have been made, unnatural trajectory generation and limited exploration of human motion uncertainties remain challenging. Because existing generative model-based methods lack reasonable guidance from motion pattern priors, and current memory-based approaches lack a systematic strategy to harness inherent uncertainties in motion pattern behavior. For instance, unexpected occurrences in real-world scenarios, like abrupt changes in human motion trajectories, are not adequately addressed and taken into consideration.

To solve these problems, we introduce a novel memory approach that combines the strengths of the aforementioned stochastic methods and memory approaches to fully leverage the valuable probabilistic information and motion pattern priors. We employ a clustering method based on the motion trend of trajectories to obtain the human motion pattern priors and store them in the memory bank, which facilitates the prediction of a novel agent’s recurring motion pattern given its observed motion state [11]. Then we retrieve the matched pattern and the potential target distribution to obtain the target priors memory token, combined with the motion state as a condition to guide the learning of the reverse diffusion process. We optimize the model using the evidence lower bound maximization method during the training, and sample the trajectories by denoising from a noise distribution during the inference. Extensive experiments validate the effectiveness of our approach, achieving state-of-the-art results on ETH/UCY and Stanford Drone datasets.

In summary, the key contributions of our work can be summarized as follows: 1) We introduce a motion pattern prior memory bank to refine prediction results. This marks the first work of utilizing a clustering method to store human motion patterns with uncertainties and target distribution priors for prediction guidance. 2) We introduce a novel target-guided diffusion model in Motion Pattern Priors Memory Network (MP²MNet). Using the matched motion pattern

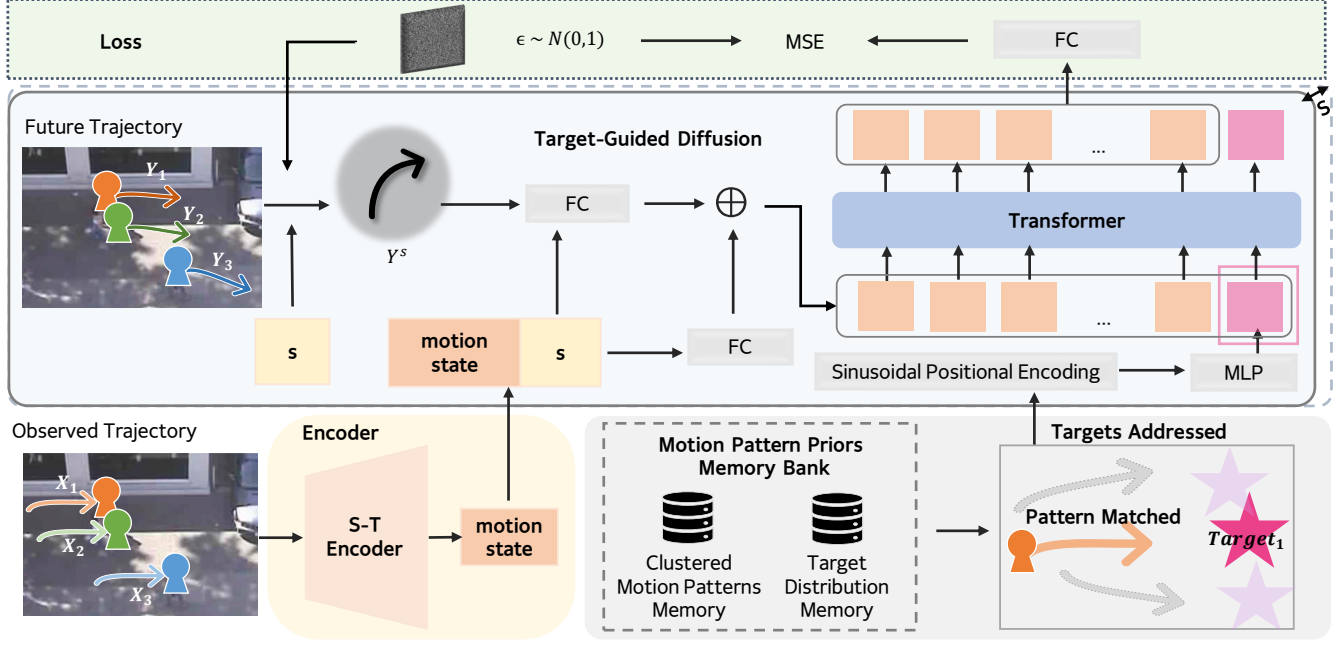


Fig. 1. The overview of our proposed MP²MNet method. It contains an encoder, the motion pattern priors memory bank, and a Transformer-based decoder. The encoder captures information to obtain the motion state representation. S denotes the total diffusion step and s denotes the s^{th} step. Y^s is corrupted s steps by adding noise variable to ground-truth Y^0 . The decoder processes Y^s along with motion state embedding, target priors memory token, and time embedding to generate the output. The training objective is to minimize the mean square error (MSE) loss between the output and the noise variable in the Gaussian distribution. This is achieved through target-guided diffusion generation for each iteration s to optimize the network.

and target distribution, we can obtain the target priors memory token as guidance for the Transformer-based decoder in the reverse diffusion process to guide the diffusion model to generate various reasonable prediction results. 3) We conduct extensive experiments on multiple benchmark datasets, showcasing the superior performance of our method compared to state-of-the-art methods from recent years.

2. RELATED WORKS

Trajectory prediction: Human trajectory prediction methods can be classified into single-modality and multi-modality approaches. In single-modality approaches, early trajectory prediction research primarily relied on deterministic models like Markov processes [12] and recurrent neural networks [13]. Nevertheless, modern approaches emphasize modeling complex social interactions among agents. For example, Social-LSTM [2] introduced a social pooling layer to capture agent interactions, extended by Social-GAN [4]. Additionally, attention-based methods are essential to capture critical interactions in crowded environments [3]. Other works have integrated scene understanding to extract global information, such as SS-LSTM [14]. Trajectron++ [5] established the connections between scene information and agent motion using graph structures, and MANTRA [15] combined

memory mechanisms with scene images. MID [8] is noteworthy as it introduced diffusion models to predict trajectories by modeling the process of human motion variation from indeterminate to determinate.

Memory Networks: Memory networks are commonly used in question-answering tasks. In recent years, memory networks have gained prominence in trajectory prediction tasks, demonstrating noteworthy advancements. Several methods have established memory repositories with diverse contents. For example, Ma et al. [16] applied memory networks to trajectory prediction tasks, utilizing generative memory for continuous trajectory prediction. Mangalam et al. [6] utilized a memory network for single-agent trajectory prediction. Similarly, SHENet [9] employed a similar approach by clustering trajectories within the same scene, filtering trajectories in the memory repository based on similarity, and utilizing multimodal information for human trajectory prediction. MemoNet [10] focuses on target points, utilizing memory mechanisms to store starting and target points and training a scoring network for target point prediction.

Different from these works, we propose a novel memory approach combining the strength of the diffusion model and using motion pattern priors to guide the trajectory generation.

3. OUR METHOD

3.1. Problem Definition

The goal of human trajectory prediction is to forecast the future trajectories of multiple agents based on their historical motion paths. Mathematically, given a scenario where the observed historical trajectories are denoted as \mathcal{Z} , and where multiple agents are present, each with their observed historical trajectory data represented as $X_i = \{x_i^t\}_{t=-T_{obs}+1}^0 \in \mathbb{R}^{T_{obs} \times 2}$, here $i \in [1, 2, \dots, N]$ represents the identifier of the observed agents in the environment, and $x_i^t \in \mathbb{R}^2$ represents the position of the i^{th} agent in the scene at time t . Our method aims to predict the trajectories of multiple agents in the future period, denoted as $Y_i = \{y_i^t\}_{t=1}^{T_{pred}} \in \mathbb{R}^{T_{pred} \times 2}$, $i \in [1, 2, \dots, N]$. The predicted future trajectories should closely resemble the ground truth as much as possible. In subsection 3.4, we denote X , Y without the agent index i for the observed and predicted trajectory.

3.2. Overall Network Architecture

We present our MP²MNet based on the diffusion model, which is a novel target-guided framework to formulate the trajectory prediction task as a reverse process of diffusion. To be specific, as depicted in Figure 1, our approach consists of three parts: 1) an encoder network, 2) a motion pattern priors memory bank, and 3) a Transformer-based decoder.

The encoder captures information from historical trajectories, producing the observed motion state embedding. Here we apply the encoder of Trajectron++ [5]. Using our motion pattern priors memory bank, we can retrieve the matched pattern and target distributions to generate target priors memory tokens as guidance. It combines with other information such as motion state embedding to serve as a condition for the Transformer-based decoder, designed to model Gaussian transitions in a Markov chain, enabling the network to optimize and generate predictions through denoising.

3.3. Motion Pattern Priors Memory

For each cluster, we utilize the **Motion Pattern Priors Memory** module to construct the memory bank \mathcal{Z}_{bank} , with clustered trajectories and uncertainty value attached. Note that, the **Motion Pattern Priors Memory** module is used to refine prediction results, which means our generative predictions do not solely rely on the memory bank. This module can be summarized as three procedures, i.e., 1) constructing the motion pattern priors memory bank, 2) retrieving the matched motion pattern with target distributions, and 3) generating corresponding target priors memory token.

Memory Bank Initialization. To efficiently improve memory usage, we utilize clustering to group similar trajectories based on their motion trends, forming clustered motion pattern distributions. These distributions are then stored in the

memory bank along with their uncertainty values. To be specific, for all trajectories in the training set, we represent their trajectories as a set \mathcal{Z} , with targets $y^{T_{pred}}$ included. Then we use K-means clustering to group similar trajectories considering the whole motion trend in the \mathcal{Z} . Assume we can obtain K clusters, representing a total of K motion pattern distribution priors, formulated as $\{\mathcal{N}\}_0^K$, of which μ_i and σ_i^2 represent 2D trajectories and uncertainty value of agent i . Corresponding target distributions of each cluster can be formulated as $\{\rho^{T_{pred}}\}_0^K$. Finally, we can obtain the motion pattern priors memory bank $\mathcal{Z}_{bank} = \{\{\mathcal{N}\}_0^K, \{\rho^{T_{pred}}\}_0^K\}$, which can be used then as priors memory.

Trajectory Addressing. Given the past trajectory X_i of agent i , we first use X_i to obtain the matched motion pattern priors \mathcal{N}_i with (μ_i, σ_i) from the memory bank by selecting the one with minimal Gaussian negative log-likelihood score.

For each motion pattern \mathcal{N}_j , assuming the provided trajectory X_i follows a Gaussian distribution with mean μ_j and variance σ_j^2 , we can calculate the Gaussian Negative Log-likelihood (NLL) score as follows:

$$S_{NLL} = \frac{1}{2} \left(\log(\max(\sigma_j, \epsilon)) + \frac{(X_i - \mu_j)^2}{\max(\sigma_j, \epsilon)} \right), \quad (1)$$

where X_i represents the provided past trajectory, μ_j corresponds to the trajectory associated with motion pattern \mathcal{N}_j stored in the memory bank, and σ_j represents the uncertainty of μ_j . The parameter ϵ is a hyper-parameter introduced for stability.

The pattern \mathcal{N}_i with μ_i and σ_i , which yields the minimum Gaussian NLL score, is considered the optimal match for the current agent i :

$$\mathcal{N}_i = \arg \min_{\mu_i, \sigma_i \in \mathcal{N}} S_{NLL}(X_i, \mu_i, \sigma_i). \quad (2)$$

Subsequently, we can retrieve the potential target distribution $\rho_i^{T_{pred}}$ associated with the matched pattern from the memory bank, which is employed to guide the diffusion process for generating future trajectories.

Target Priors Memory Token Generation. Using the obtained potential target distribution $\rho_i^{T_{pred}}$ of the agent i through the trajectory addressing mechanism, we use sinusoidal position encoding and MLP to convert 2D target positions into target embedding, used as an additional target prior for prediction refinement:

$$\begin{aligned} \mathbf{h}_{2j} &= f(\sin(\rho_i^{T_{pred}} / \lambda^{2j/D})), \\ \mathbf{h}_{2j+1} &= f(\cos(\rho_i^{T_{pred}} / \lambda^{2j/D})), \end{aligned} \quad (3)$$

where $\rho_i^{T_{pred}}$ represents the target position of agent i , $\mathbf{h} \in \mathbb{R}^D$ represents the target priors memory token, j is the dimension index, and D is the dimension of the embedding $\rho_i^{T_{pred}}$. λ

Table 1. Quantitative results on the Stanford Drone dataset with Best-of-20 strategy in ADE/FDE metric. \downarrow represents that lower is better. The best results are highlighted in bold.

Time	Social-LSTM [2]	Social-GAN [4]	Trajectron++ [5]	MANTRA [15]	GroupNet+CVAE [7]	MP ² MNet
4.8s	31.19/56.97	27.23/41.44	19.30/32.70	8.96/17.76	9.31/ 16.11	8.89 /16.45

denotes the max period of the sinusoidal function. The wave-lengths form a geometric progression from 2π to $10000 \cdot 2\pi$. And $f(\cdot)$ denotes MLP.

3.4. Target-guided Diffusion Model

As depicted in Figure 1, we utilize the Transformer as the decoder following the previous work [8]. We denote that \mathbf{Y}^s is corrupted by adding a noise variable for s times to the ground truth trajectory \mathbf{Y}^0 .

Then we take \mathbf{Y}^s , the target priors memory token \mathbf{h} combined with the motion state embedding denoted as \mathbf{G} , and time embedding as the input of the Transformer-based decoder for the reverse diffusion process.

The decoder is trained to generate trajectories from Gaussian noise conditioned on the information including \mathbf{G} at each step of the denoising process. The reverse diffusion process progressively diminishes uncertainties across all accessible regions, ultimately leading to specific predictions using a parameterized Markov chain.

Target-guided Diffusion. The reverse diffusion process is the joint distribution $p_\theta(\mathbf{Y}^{(0:S)} | \mathbf{G})$ conditioned on \mathbf{G} , defined as a Markov chain with learned Gaussian transitions that begins with $p(\mathbf{Y}^S) = \mathcal{N}(\mathbf{Y}^S; \mathbf{0}, \mathbf{I})$:

$$p_\theta(\mathbf{Y}^{(0:S)}) := p(\mathbf{Y}^S) \prod_{s=1}^S p_\theta(\mathbf{Y}^{s-1} | \mathbf{Y}^s, \mathbf{G}), \quad (4)$$

$$p_\theta(\mathbf{Y}^{s-1} | \mathbf{Y}^s, \mathbf{G}) := \mathcal{N}(\mathbf{Y}^{s-1}; \boldsymbol{\mu}_\theta(\mathbf{Y}^s, s, \mathbf{G}), \boldsymbol{\Sigma}_\theta(\mathbf{Y}^s, s)), \quad (5)$$

where s denotes the diffusion step, θ represents our target-guided diffusion model’s parameter, and $\boldsymbol{\Sigma}_\theta(\mathbf{Y}^s, s)$ equals to $\beta_s \mathbf{I}$. β_s is the variance at the denoising step s , controlling the extent of added noise.

The forward diffusion process is a Markov chain that gradually adds Gaussian noise to raw trajectory data for S steps according to a uniformly increasing variance schedule β_1, \dots, β_S , which constrains the level of noise injection. We can formulate the approximate posterior as:

$$q(\mathbf{Y}^{(1:S)} | \mathbf{Y}^0) := \prod_{s=1}^S q(\mathbf{Y}^s | \mathbf{Y}^{s-1}), \quad (6)$$

$$q(\mathbf{Y}^s | \mathbf{Y}^{s-1}) = \mathcal{N}(\mathbf{Y}^s; \sqrt{1 - \beta_s} \mathbf{Y}^{s-1}, \beta_s \mathbf{I}). \quad (7)$$

Using the notation $\alpha_s := 1 - \beta_s$ and $\bar{\alpha}_s := \prod_{m=1}^s \alpha_m$, we can obtain:

$$q(\mathbf{Y}^s | \mathbf{Y}^0) = \mathcal{N}(\mathbf{Y}^s; \sqrt{\bar{\alpha}_s} \mathbf{Y}^0, (1 - \bar{\alpha}_s) \mathbf{I}). \quad (8)$$

When the total number of denoising step S is large enough, $q(\mathbf{Y}^S)$ approximates to $\mathcal{N}(\mathbf{Y}^S; \mathbf{0}, \mathbf{I})$, where \mathcal{N} is a Gaussian distribution.

Training Objective. Our target-guided diffusion model performs training by optimizing the variational lower bound. As the exact log-likelihood is intractable, we use the evidence lower bound maximization method and minimize the KL divergence. We can use KL divergence to directly compare $p_\theta(\mathbf{Y}^{s-1} | \mathbf{Y}^s, \mathbf{G})$ against forward process posteriors:

$$\begin{aligned} \mathcal{L} &= \mathbb{E}_{q,s} [D_{KL}(q(\mathbf{Y}^{s-1} | \mathbf{Y}^s, \mathbf{Y}^0) \| p_\theta(\mathbf{Y}^{s-1} | \mathbf{Y}^s, \mathbf{G}))] \\ &= \mathbb{E}_{q,s} [D_{KL}(\mathcal{N}(\mathbf{Y}^{s-1}; \tilde{\boldsymbol{\mu}}_s, \boldsymbol{\Sigma}_q(s)) \| \mathcal{N}(\mathbf{Y}^{s-1}; \boldsymbol{\mu}_\theta, \boldsymbol{\Sigma}_{(s)}))] \\ &= \mathbb{E}_{q,s} [\|\boldsymbol{\mu}_\theta(\mathbf{Y}^s, s, \mathbf{G}) - \tilde{\boldsymbol{\mu}}_s\|_2^2], \end{aligned} \quad (9)$$

where $\boldsymbol{\mu}_\theta$ and $\tilde{\boldsymbol{\mu}}_s$ are calculated using the reparameterization trick as:

$$\begin{aligned} \tilde{\boldsymbol{\mu}}_s(\mathbf{Y}^s, \mathbf{Y}^0) &= \frac{\sqrt{\bar{\alpha}_{s-1}} \beta_s}{1 - \bar{\alpha}_s} \mathbf{Y}^0 + \frac{\sqrt{\alpha_s} (1 - \bar{\alpha}_{s-1})}{1 - \bar{\alpha}_s} \mathbf{Y}^s, \\ \tilde{\beta}_s &= \frac{1 - \bar{\alpha}_{s-1}}{1 - \bar{\alpha}_s} \beta_s \mathbf{I}, \end{aligned} \quad (10)$$

$$\boldsymbol{\mu}_\theta(\mathbf{Y}^s, s, \mathbf{G}) = \frac{1}{\sqrt{\alpha_s}} \left(\mathbf{Y}^s - \frac{\beta_s}{\sqrt{1 - \alpha_s}} \epsilon_\theta(\mathbf{Y}^s, s, \mathbf{G}) \right), \quad (11)$$

where $\epsilon_\theta(\cdot)$ denotes the noise predictor of our target-guided diffusion model for trajectory generation. We optimize the network through diffusion generation by performing mean square error (MSE) loss between the output and a noise variable in standard Gaussian distribution for the current iteration s , following the work [8]:

$$\mathcal{L}_{MSE}(\theta, \phi) = \mathbb{E}_{\mathbf{z}, \mathbf{Y}^0, s} \|\mathbf{z} - \epsilon_{(\theta, \phi)}(\mathbf{Y}^s, s, \mathbf{G})\|, \quad (12)$$

where θ and ϕ are parameters of the target-guided diffusion model and encoder respectively, and $\mathbf{z} \sim ((\mathbf{0}, \mathbf{I}))$.

Inference. During the reverse process, with the reparameterization, we use the DDPM sampling technique to repeatedly denoise \mathbf{Y}^S to \mathbf{Y}^0 by using the equation below for S steps as:

$$\mathbf{Y}^{s-1} = \frac{1}{\sqrt{\alpha_s}} \left(\mathbf{Y}^s - \frac{\beta_s}{\sqrt{1 - \alpha_s}} \epsilon_\theta(\mathbf{Y}^s, s, \mathbf{G}) \right) + \sqrt{\beta_s} \mathbf{z}. \quad (13)$$

4. EXPERIMENTS

4.1. Experimental Setup

Datasets. We evaluate the effectiveness of our MP²MNet on two commonly used benchmarks for human trajectory

Table 2. Comparison of state-of-the-art methods on ETH/UCY datasets. \downarrow represents that lower is better. We report ADE and FDE for predicting future 12 frames in meters. \dagger represents our reproduction results. ‘AVG’ means the average result over 5 subsets. The best-of-20 is adopted for evaluation. The best results are highlighted in bold while the second-best results are underlined.

Methods	Evaluation metrics: ADE \downarrow / FDE \downarrow (in meters)					
	ETH	HOTEL	UNIV	ZARA1	ZARA2	AVG
LSTM	1.01 / 1.94	0.60 / 1.34	0.71 / 1.52	0.41 / 0.89	0.31 / 0.68	0.61 / 1.27
S-LSTM [2]	0.75 / 1.38	0.61 / 1.40	0.58 / 1.03	0.42 / 0.70	0.43 / 0.71	0.56 / 1.05
SGAN [4]	0.87 / 1.62	0.67 / 1.37	0.76 / 1.52	0.35 / 0.68	0.42 / 0.84	0.61 / 1.21
STGAT [3]	0.68 / 1.33	0.38 / 0.72	0.56 / 1.21	0.34 / 0.69	0.29 / 0.60	0.45 / 0.91
MANTRA [15]	0.70 / 1.76	0.28 / 0.68	0.51 / 1.26	0.25 / 0.67	0.20 / 0.54	0.39 / 0.98
TPNMS [17]	0.52 / 0.89	0.22 / 0.39	0.55 / 1.13	0.35 / 0.70	0.27 / 0.56	0.38 / 0.73
Social-Implicit [18]	0.66 / 1.44	0.20 / 0.36	0.31 / 0.60	0.25 / 0.50	0.22 / 0.43	0.33 / 0.67
GroupNet [7]	0.46 / <u>0.73</u>	0.15 / 0.25	0.26 / 0.49	<u>0.21</u> / 0.39	<u>0.17</u> / <u>0.33</u>	<u>0.25</u> / 0.44
MID \dagger [8]	<u>0.42</u> / 0.75	0.18 / 0.32	<u>0.23</u> / <u>0.46</u>	0.20 / <u>0.40</u>	<u>0.17</u> / 0.34	<u>0.25</u> / 0.46
Ours (w/o memory)	0.44 / 0.76	0.18 / 0.33	<u>0.23</u> / 0.47	0.25 / 0.52	0.19 / 0.41	0.26 / 0.50
Ours (w/ memory)	0.39 / 0.69	<u>0.16</u> / <u>0.27</u>	0.21 / 0.43	0.23 / 0.48	0.16 / 0.32	0.23 / 0.44

prediction tasks: ETH/UCY [19, 20], and Stanford Drone Dataset(SDD) [21]. ETH/UCY includes positions of pedestrians in the world coordinates from 5 scenes: ETH, HOTEL, UNIV, ZARA1, and ZARA2. We evaluate our model on this dataset using the same approach as in previous works [4, 3], employing the leave-one-out method. SDD is captured in a university campus environment from a bird’s-eye view. For both datasets, we use the data from the past 8 frames (3.2 seconds) to predict the trajectory for the future 12 frames (4.8 seconds).

Evaluation Metrics. Evaluation metrics include ADE and FDE, which are commonly used in prior works: Average Displacement Error (ADE) measures the average L2 distance between the ground truth and prediction results over all specified prediction time steps, while Final Displacement Error (FDE) represents the distance between the predicted destination and the true destination at time-step T_{pred} .

Implementation Details. The training was performed with Adam Optimizer with a learning rate of 0.001 and a batch size of 256. We set diffusion steps S as 100. The Transformer has three layers with 512 dimensions and four attention heads. The final trajectory prediction is obtained by downsampling the Transformer output sequence through three fully connected layers (from 512d to 256d and then to 2d).

4.2. Results and Analysis

Validation Results on Pedestrian Datasets. We conduct a comprehensive quantitative comparison of our MP²MNet method with a diverse set of contemporary approaches. We adopt a best-of-20 evaluation strategy, consistent with previ-

ous methods [4, 3, 7, 8] for fair comparison.

Table 1 provides a comparison between our method and typical existing approaches on the Stanford Drone Dataset. Our method achieves a leading average ADE of 8.89 in pixel coordinates, surpassing all prevalent approaches. Meanwhile, our method achieved the best mean ADE/FDE (0.23/0.44) for the ETH/UCY dataset, outperforming all other trajectory prediction methods. Detailed quantitative results comparing our proposed method with state-of-the-art methods are presented in Table 2. Our method exhibits superior performance, demonstrating an 8% reduction in ADE compared to the state-of-the-art GroupNet. Compared to MID [8], our method achieves improvements in both ADE and FDE in the ETH scene, with reductions of 7% and 8% respectively. Notably, our model exhibits significant advancements over previous methods, particularly in the ETH, UNIV, and ZARA2.

Ablation Study. Furthermore, we explore the impact of our motion pattern priors memory bank. We substitute the target priors memory token to the raw predicted target embedding for comparison. Comparisons of the last two rows of Table 2 and the visualization results in Fig. 2 (b) and (c) reveal that our memory-based approach enhances prediction performance. Our method with motion pattern priors memory outperforms the method without this memory by reducing mean ADE by 11.5% and mean FDE by 12%.

Visualization Results. Visualization results for comparison are tested on scenes in the ETH/UCY dataset, as shown in Fig. 2. To validate the effectiveness of our memory approach, we compare the prediction results of our method and two other baseline methods including MID [8] and our method without motion pattern priors memory. Our method

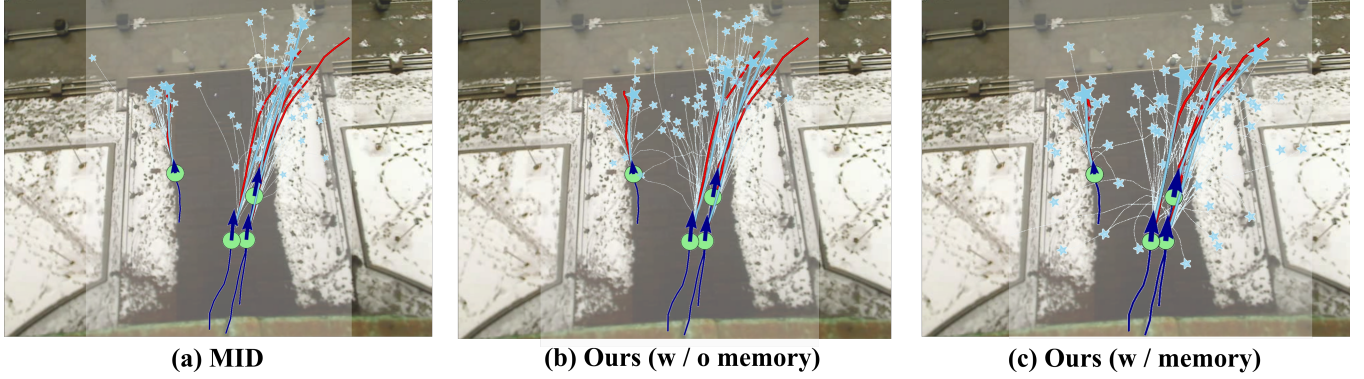


Fig. 2. Visualization comparison on the ETH/UCY datasets. We compare the best-of-20 predictions generated by our approach with those from two baseline methods: the previous MID method [8] and our method without the motion pattern priors memory. Ground truths are in red solid lines, past trajectories in dark blue solid lines, and prediction results in light blue lines. We visualize 20 predictions for each agent with light blue dashed lines and corresponding targets are marked with stars. The result shows significant improvements by utilizing our memory-based method.

has been proven to be effective based on the qualitative evaluation results. The best-of-20 prediction results are closest to the ground truth, and the predictions fall within a reasonable diverse range, which retains stochastic varieties of human movements and considers diverse human motion patterns.

5. CONCLUSION

In this paper, we propose a novel memory approach to efficiently leverage motion pattern priors from the training set. We introduce a cluster-based memory bank to store human motion patterns with target distributions. We adopt an addressing mechanism to retrieve the matched pattern and the target distribution and generate the target priors memory token which in turn guides the diffusion model to generate trajectories. Extensive experiments and the ablation study validate the effectiveness of our method.

6. REFERENCES

- [1] Jesse Levinson, Jake Askeland, Jan Becker, Jennifer Dolson, David Held, Soeren Kammel, J Zico Kolter, Dirk Langer, Oliver Pink, Vaughan Pratt, et al., “Towards fully autonomous driving: Systems and algorithms,” in *2011 IEEE intelligent vehicles symposium (IV)*. IEEE, 2011, pp. 163–168.
- [2] Alexandre Alahi, Kratharth Goel, Vignesh Ramanathan, Alexandre Robicquet, Li Fei-Fei, and Silvio Savarese, “Social lstm: Human trajectory prediction in crowded spaces,” in *CVPR*, 2016, pp. 961–971.
- [3] Yingfan Huang, Huikun Bi, Zhaoxin Li, Tianlu Mao, and Zhaoqi Wang, “Stgat: Modeling spatial-temporal interactions for human trajectory prediction,” in *CVPR*, 2019, pp. 6272–6281.
- [4] Agrim Gupta, Justin Johnson, Li Fei-Fei, Silvio Savarese, and Alexandre Alahi, “Social gan: Socially acceptable trajectories with generative adversarial networks,” in *CVPR*, 2018, pp. 2255–2264.
- [5] Tim Salzmann, Boris Ivanovic, Punarjay Chakravarty, and Marco Pavone, “Trajectron++: Dynamically-feasible trajectory forecasting with heterogeneous data,” in *ECCV*. Springer, 2020, pp. 683–700.
- [6] Karttikeya Mangalam, Harshayu Girase, Shreyas Agarwal, Kuan-Hui Lee, Ehsan Adeli, Jitendra Malik, and Adrien Gaidon, “It is not the journey but the destination: Endpoint conditioned trajectory prediction,” in *ECCV*. Springer, 2020, pp. 759–776.
- [7] Chenxin Xu, Maosen Li, Zhenyang Ni, Ya Zhang, and Siheng Chen, “Groupnet: Multiscale hypergraph neural networks for trajectory prediction with relational reasoning,” in *CVPR*, 2022, pp. 6498–6507.
- [8] Tianpei Gu, Guangyi Chen, Junlong Li, Chunze Lin, Yongming Rao, Jie Zhou, and Jiwen Lu, “Stochastic trajectory prediction via motion indeterminacy diffusion,” in *CVPR*, 2022, pp. 17113–17122.
- [9] Mancheng Meng, Ziyan Wu, Terrence Chen, Xiran Cai, Xiang Zhou, Fan Yang, and Dinggang Shen, “Forecasting human trajectory from scene history,” *NeurIPS*, vol. 35, pp. 24920–24933, 2022.
- [10] Chenxin Xu, Weibo Mao, Wenjun Zhang, and Siheng Chen, “Remember intentions: retrospective-memory-based trajectory prediction,” in *CVPR*, 2022, pp. 6488–6497.
- [11] Judith A Ouellette and Wendy Wood, “Habit and intention in everyday life: The multiple processes by which past behavior predicts future behavior,” *Psychological bulletin*, vol. 124, no. 1, pp. 54, 1998.
- [12] Ankit Kumar, Ozan Irsoy, Peter Ondruska, Mohit Iyyer, James Bradbury, Ishaan Gulrajani, Victor Zhong, Romain Paulus, and Richard Socher, “Ask me anything: Dynamic memory networks for natural language processing,” in *ICML*. PMLR, 2016, pp. 1378–1387.
- [13] Jeremy Morton, Tim A Wheeler, and Mykel J Kochenderfer, “Analysis of recurrent neural networks for probabilistic modeling of driver behavior,” *TITS*, vol. 18, no. 5, pp. 1289–1298, 2016.
- [14] Hao Xue, Du Q Huynh, and Mark Reynolds, “Ss-lstm: A hierarchical lstm model for pedestrian trajectory prediction,” in *WACV*. IEEE, 2018, pp. 1186–1194.
- [15] Francesco Marchetti, Federico Becattini, Lorenzo Seidenari, and Alberto Del Bimbo, “Mantra: Memory augmented networks for multiple trajectory prediction,” in *CVPR*, 2020, pp. 7143–7152.
- [16] Hengbo Ma, Yaofeng Sun, Jiachen Li, Masayoshi Tomizuka, and Chihoi Choi, “Continual multi-agent interaction behavior prediction with conditional generative memory,” *RAL*, vol. 6, no. 4, pp. 8410–8417, 2021.
- [17] Rongqin Liang, Yuanman Li, Xia Li, Yi Tang, Jiantao Zhou, and Wenbin Zou, “Temporal pyramid network for pedestrian trajectory prediction with multi-supervision,” in *AAAI*, 2021, vol. 35, pp. 2029–2037.
- [18] Abdullh Mohamed, Deyao Zhu, Warren Vu, Mohamed Elhoseiny, and Christian Claudel, “Social-implicit: Rethinking trajectory prediction evaluation and the effectiveness of implicit maximum likelihood estimation,” in *ECCV*. Springer, 2022, pp. 463–479.

- [19] Stefano Pellegrini, Andreas Ess, and Luc Van Gool, "Improving data association by joint modeling of pedestrian trajectories and groupings," in *ECCV*. Springer, 2010, pp. 452–465.
- [20] Alon Lerner, Yiorgos Chrysanthou, and Dani Lischinski, "Crowds by example," in *Computer graphics forum*. Wiley Online Library, 2007, vol. 26, pp. 655–664.
- [21] Alexandre Robicquet, Amir Sadeghian, Alexandre Alahi, and Silvio Savarese, "Learning social etiquette: Human trajectory understanding in crowded scenes," in *ECCV*. Springer, 2016, pp. 549–565.